
# Barracuda Application Models: Overview, Hydrogen Production and Liquid Slurry Flows

Shashank Karra, PhD

CPFD Software

June 25, 2026

# What is a Barracuda Virtual Reactor Application Model?

**Application models are sample cases that can by downloaded, run, and customized by the Barracuda Virtual Reactor user community**

- Available on cpfd-software.com

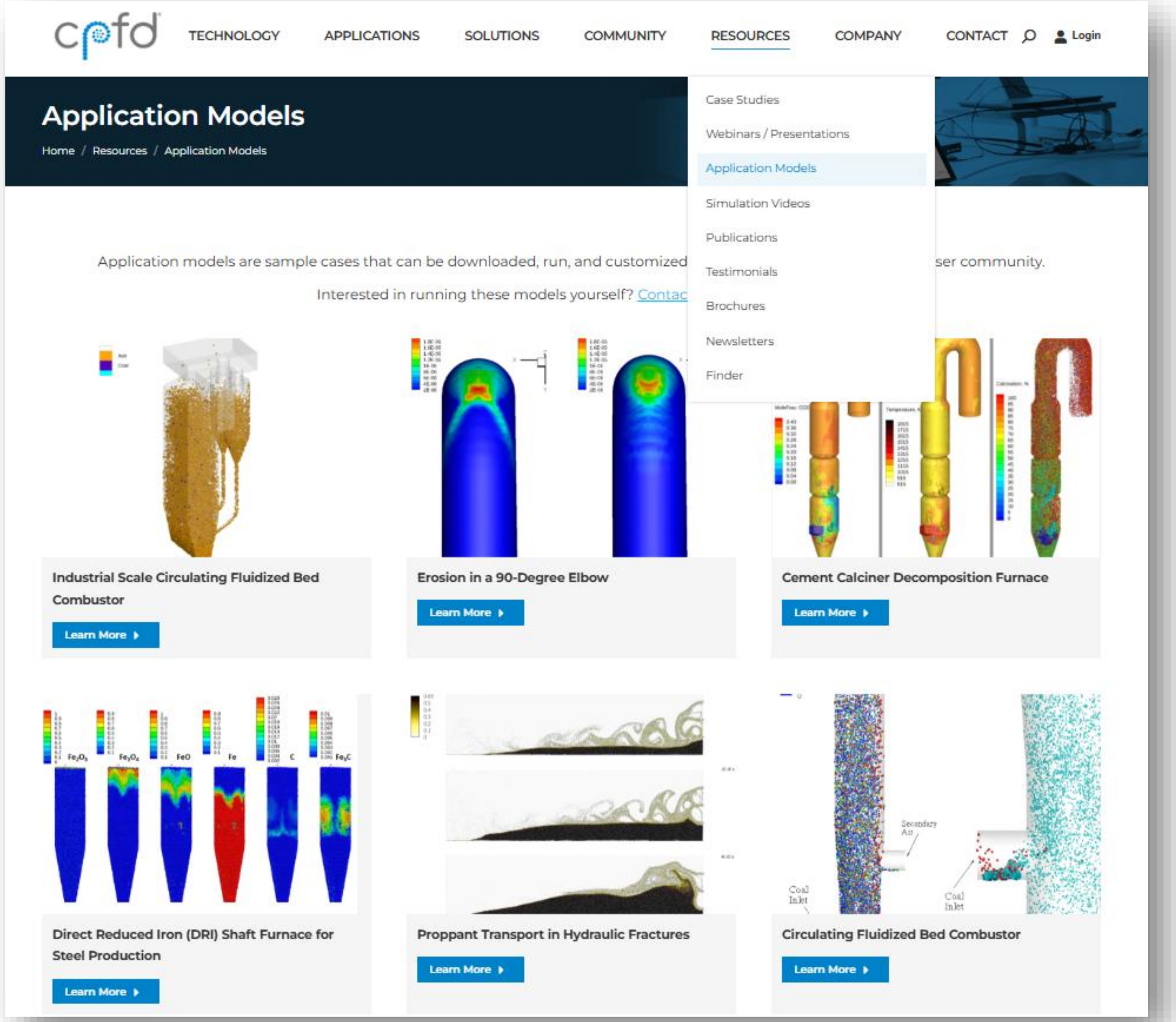


Direct URL: https://cpfd-software.com/resource/application-models/

# Why Application Models?

**Application models supplement other information on applications:**

- Publications – The application is possible to model
- Case studies – Others have modeled the application
- Application models – You can model it yourself!

**Application models are useful for:**

- Demonstration cases / software trials
- Supplementing new user training – Train new employees
- Starting point for setting up your own systems

**Translating features into action – Bridge the gap between what the software can do and what the user needs to do**

# What Does an Application Model Include?

**Application models include the following:**

- Application overview
- Model description and definition
- Reaction kinetics (if applicable)
- Results and discussion
- Modeling instructions (with downloadable project files*)
- Post-processing instructions
- References

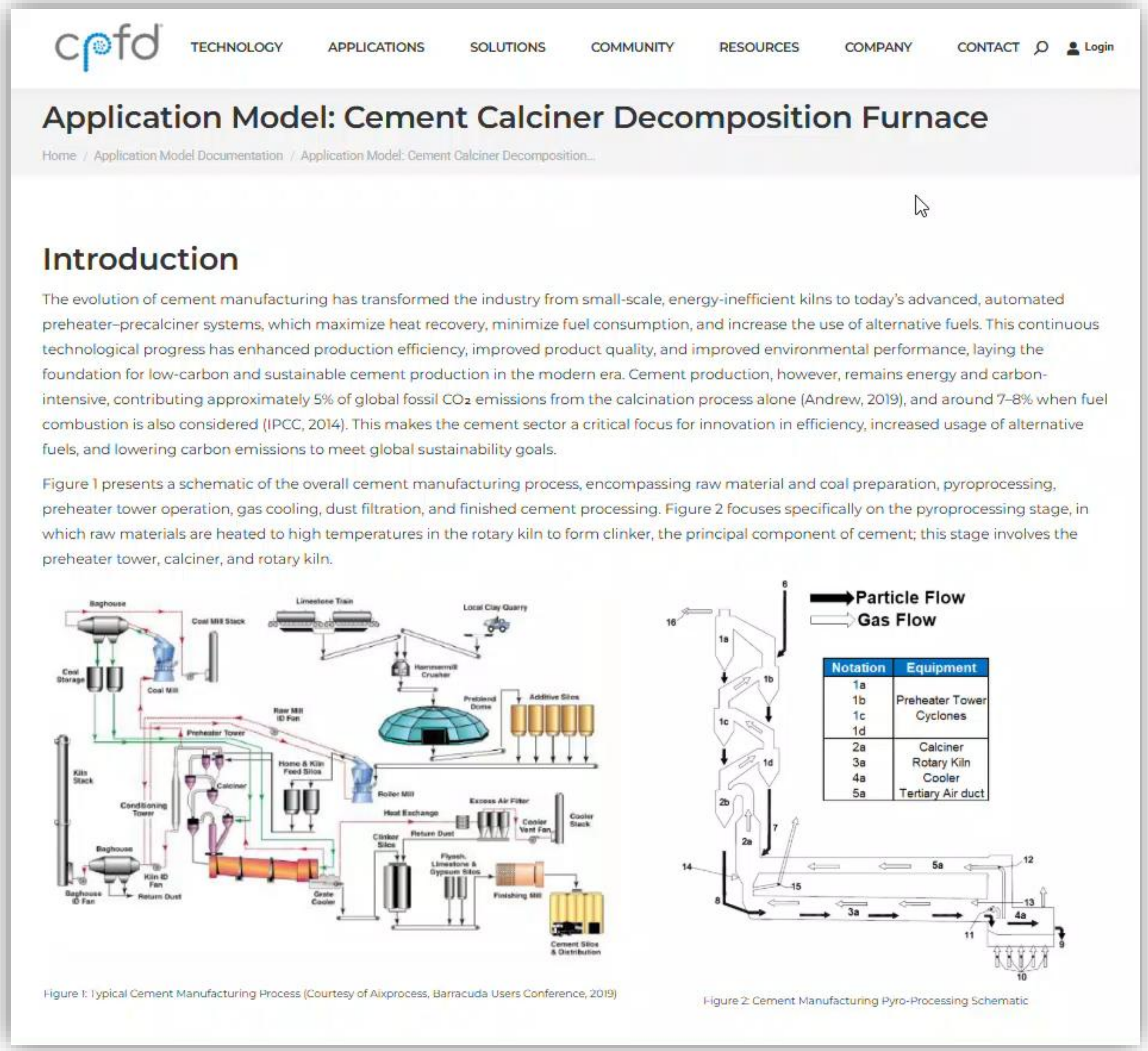
cpfd TECHNOLOGY APPLICATIONS SOLUTIONS COMMUNITY RESOURCES COMPANY CONTACT Login

Application Model: Cement Calciner Decomposition Furnace

Home / Application Model Documentation / Application Model: Cement Calciner Decomposition...

Introduction

The evolution of cement manufacturing has transformed the industry from small-scale, energy-inefficient kilns to today's advanced, automated preheater–precalciner systems, which maximize heat recovery, minimize fuel consumption, and increase the use of alternative fuels. This continuous technological progress has enhanced production efficiency, improved product quality, and improved environmental performance, laying the foundation for low-carbon and sustainable cement production in the modern era. Cement production, however, remains energy and carbon-intensive, contributing approximately 5% of global fossil $CO_2$ emissions from the calcination process alone (Andrew, 2019), and around 7–8% when fuel combustion is also considered (IPCC, 2014). This makes the cement sector a critical focus for innovation in efficiency, increased usage of alternative fuels, and lowering carbon emissions to meet global sustainability goals.

Figure 1 presents a schematic of the overall cement manufacturing process, encompassing raw material and coal preparation, pyroprocessing, preheater tower operation, gas cooling, dust filtration, and finished cement processing. Figure 2 focuses specifically on the pyroprocessing stage, in which raw materials are heated to high temperatures in the rotary kiln to form clinker, the principal component of cement; this stage involves the preheater tower, calciner, and rotary kiln.



Figure 1: Typical Cement Manufacturing Process (Courtesy of Aixprocess, Barracuda Users Conference, 2019)

Figure 2: Cement Manufacturing Pyro-Processing Schematic

* Support site login required for project file download.

# Application Models Demonstrations

## Todays Topics

- **Hydrogen Production**
  - Sorbent enhanced Steam Methane Reforming (SE-SMR)
  - Dry Reforming of Methane (DRM)
  - Molten Metal Bubble Column Reactor (MMBCR)
- **Demo**
- **Liquid Slurry Flows in Oil & Gas Applications**

# Hydrogen Production

# Advancing Low-Carbon Hydrogen Production

**Hydrogen is a critical energy carrier for meeting GHG reduction targets, requiring a rapid transition from carbon-intensive Grey hydrogen to cleaner Blue and Green pathways**

- Diverse Pathways
  - Advanced reforming utilizing fluidized bed reactors to couple complex chemistry with in-situ $CO_2$ capture or sustainable waste-to-energy feedstocks
    - Sorbent enhanced steam methane reforming (SE-SMR)
    - Dry reforming of methane (DRM)
    - Methane Pyrolysis (MMBCR): Leveraging molten metal bubble columns to thermally decompose methane into $H_2$ and solid carbon, inherently bypassing $CO_2$ formation.
- The CPFD Advantage: Barracuda Virtual Reactor enables the optimization of these emerging technologies by resolving the complex gas-solid-liquid hydrodynamics coupled with chemical reactions that dictate reactor efficiency

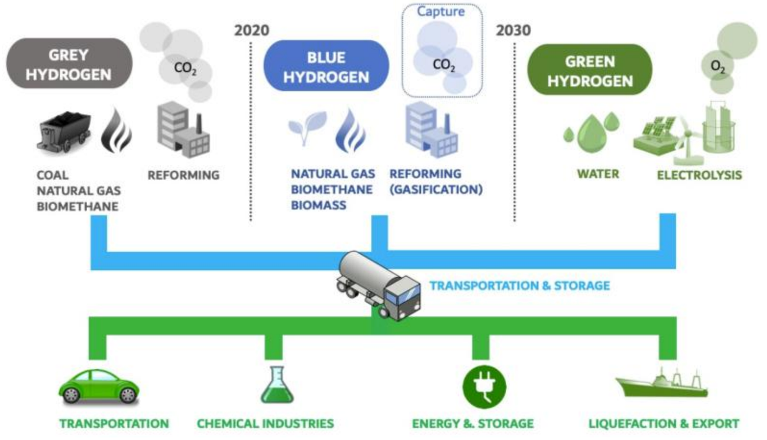


Ref: https://www.chem4us.be/blue-green-gray-the-colors-of-hydrogen/

# Hydrogen Production with Sorbent enhanced Steam Methane Reforming (SE-SMR)

**Simulate a bubbling fluidized bed SE-SMR reactor to evaluate in-situ $CO_2$ capture, targeting maximized $H_2$ yield by integrating production with pre-combustion carbon capture** (*based on work of Johnston et. al.*)

- Barracuda Virtual Reactor Solution
  - Reactive MP-PIC model capturing gas - solid hydrodynamics, interphase interactions, and sorbent behavior
  - Coupled physics and chemistry - gas turbulence, heat/mass transfer, and both homogeneous & heterogeneous reactions
  - Dynamic $CO_2$ capture modeling integrated with reactor operation
- Value of Simulation
  - Optimize reactor design and scale-up from lab to commercial scale
  - Maximize $H_2$ yield by evaluating operating strategies and sorbent performance
  - Reveal internal reactor behavior not measurable in experiments

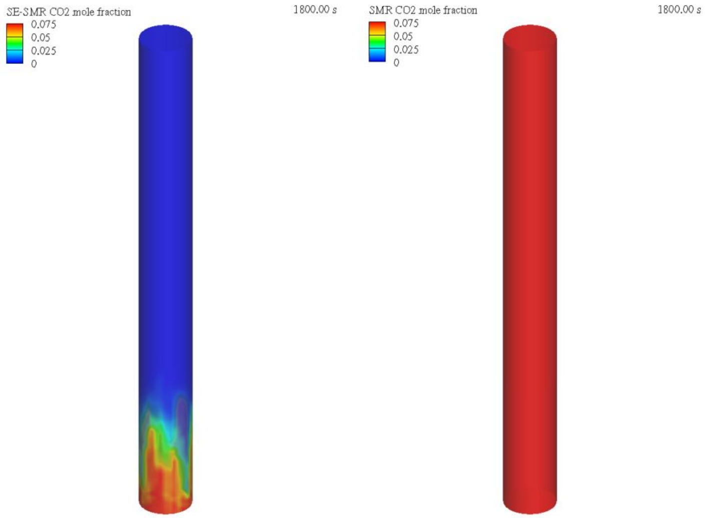

# Hydrogen Production with SE-SMR

- Cylindrical Reactor Domain
  - Based on work by Jonston et. al
  - Ni-based catalyst; Calcined Dolomite sorbent (ratio = 2.44)
  - Gas velocity = 3.2e-2 m/s
- Chemistry
  - Steam methane reforming and water gas shift reactions

$$SMR: CH_4 + H_2O \iff CO + 3H_2$$

$$SMR: CH_4 + 2H_2O \iff CO_2 + 4H_2$$

$$WGS: CO + H_2O \iff CO_2 + H_2$$

  - Discrete carbonation reaction

$$CaO + CO_2 \iff CaCO_3$$

  - Kinetics: Homogenous and Discrete reaction rate expressions

$$R_1 = \frac{k_1}{p_{H_2}^{2.5}(DEN)^2}\left(P_{CH_4}P_{H_2O} - \frac{P_{H_2}^3 P_{CO}}{K_I}\right)$$

$$R_2 = \frac{k_2}{p_{H_2}^{3.5}(DEN)^2}\left(P_{CH_4}P_{H_2O}^2 - \frac{P_{H_2}^4 P_{CO_2}}{K_{II}}\right)$$

$$R_3 = \frac{k_3}{p_{H_2}(DEN)^2}\left(P_{CO}P_{H_2O} - \frac{P_{H_2} P_{CO_2}}{K_{III}}\right)$$

$$DEN = 1 + K_{CO}P_{CO} + K_{H_2}P_{H_2} + K_{CH_4}P_{CH_4} + \frac{K_{H_2O}P_{H_2O}}{P_{H_2}}$$

$$r_{carb} = k_{carb}\left(p_{CO_2} - p_{CO_{2,eq}}\right)^n S_0 \left(1 - X_{CaO}\right)$$

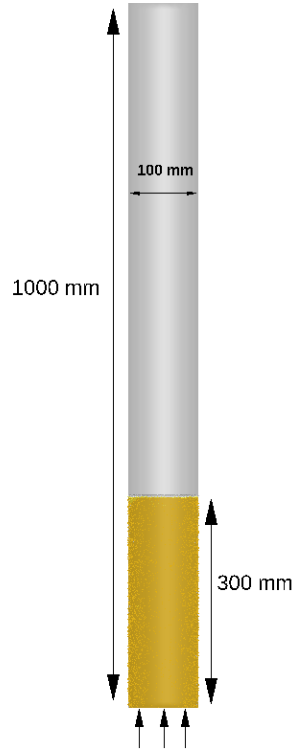


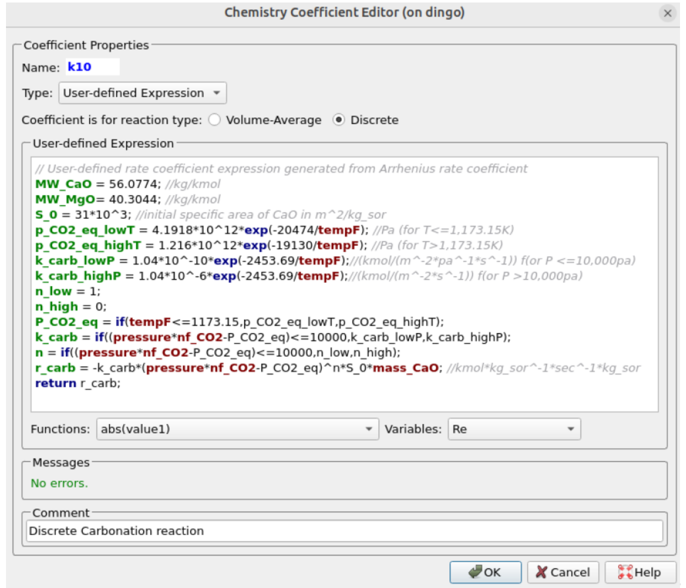

# Hydrogen Production with SE-SMR

## Animation shows $CO_2$ distribution comparison

- Regular SMR vs. SE-SMR
- Dolomite sorbent captures produced $CO_2$ within the reactor, shifting equilibrium toward higher $H_2$ yield

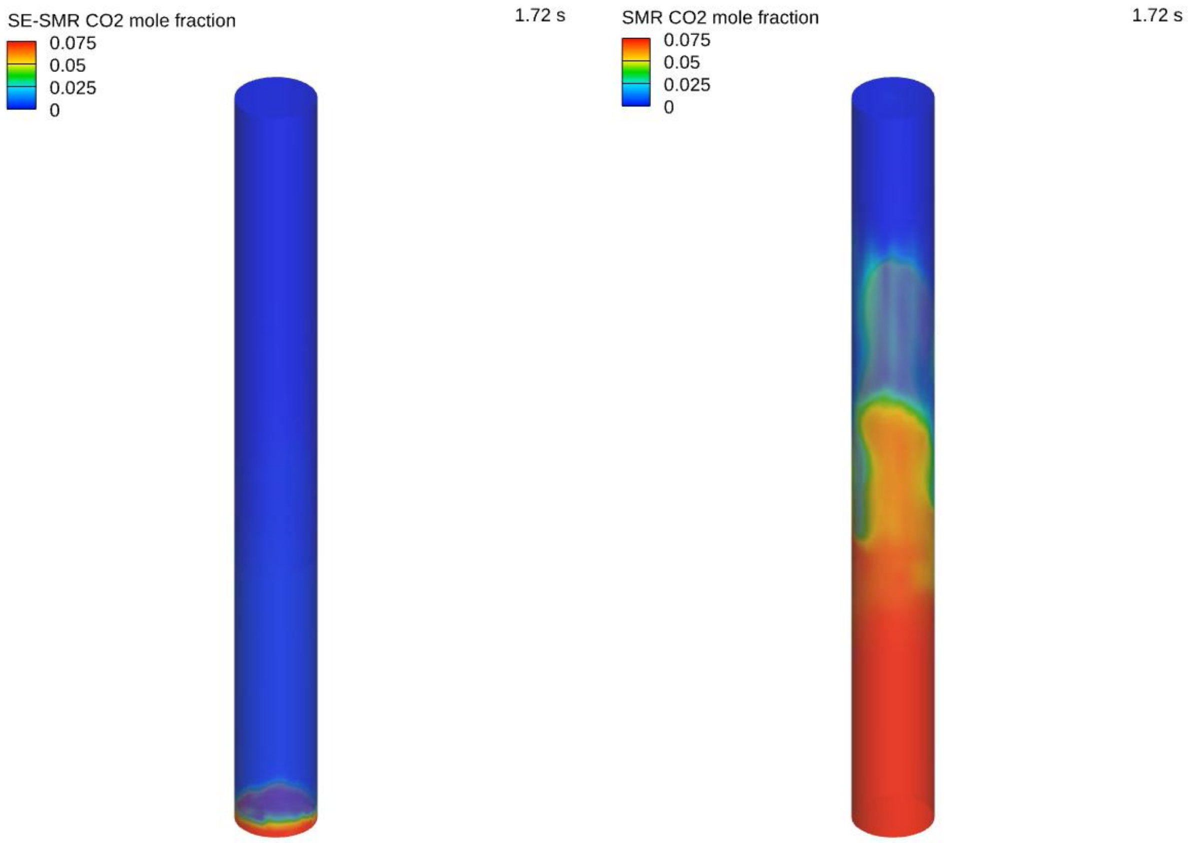


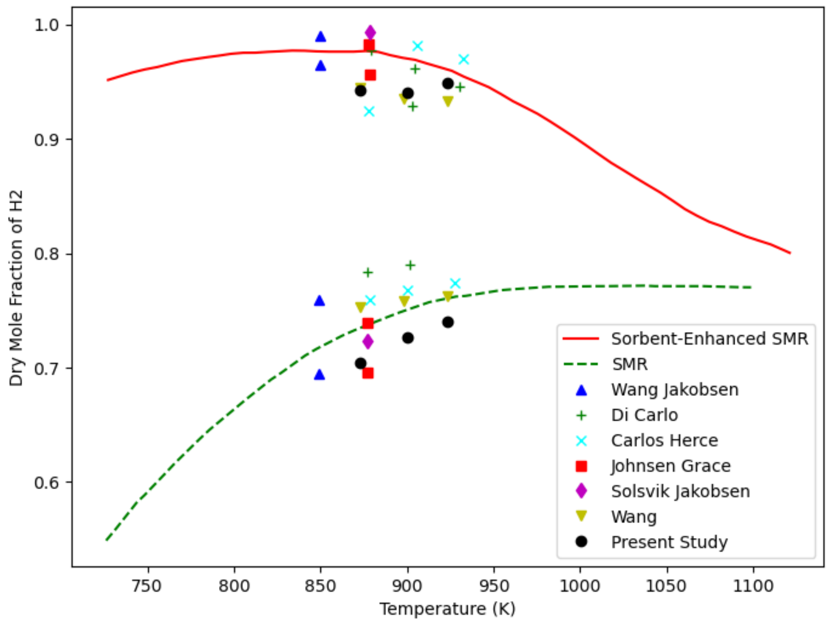


$H_2$ outlet mole fraction benchmarked against results from literature

# Hydrogen Production with Dry Reforming of Methane (DRM)

**Simulate a fluidized bed DRM reactor to evaluate syngas production from biogas, targeting the conversion of major greenhouse gases ($CH_4$ and $CO_2$) into high-value hydrogen and CO** (*based on work of Ugarte et al.)*

- Barracuda Virtual Reactor Solution
  - Reactive MP-PIC model capturing gas-solid hydrodynamics, interphase interactions, and sorbent behavior
  - Coupled physics and chemistry - gas turbulence, heat/mass transfer, and homogeneous reactions
  - Conversion of $CH_4$ and $CO_2$ into syngas products, namely CO and $H_2$ captured dynamically
- Value of Simulation
  - Maximize syngas yield by testing operating strategies, feed ratios and thermal management

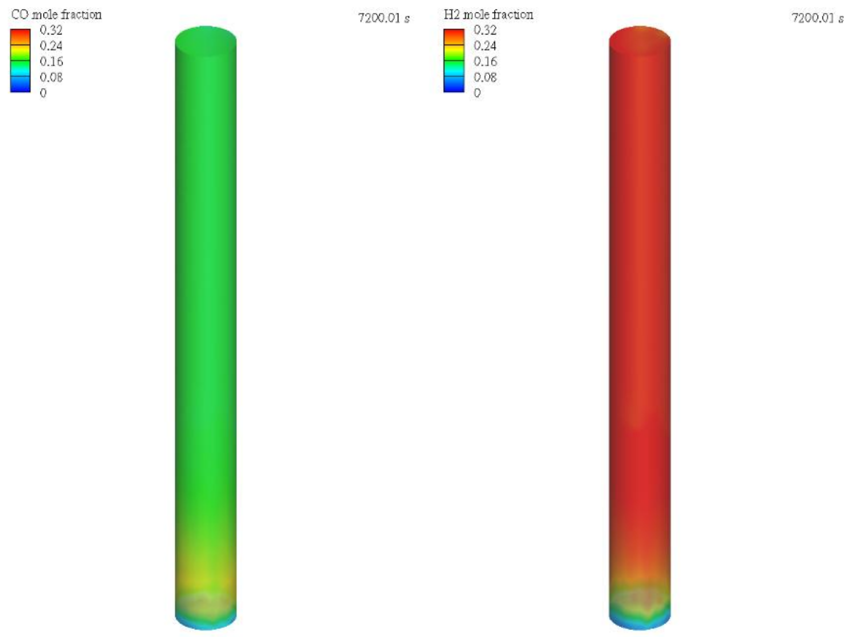

# Hydrogen Production with DRM

- Cylindrical Reactor Domain
  - Ni-based catalyst; CH4:CO:Ar at a molar ratio of 4:4:2
  - Gas velocity = 1.22e-2 m/s
- Chemistry
  - Dry reforming of methane, reverse water gas shift, methane decomposition, steam gasification and Boudouard reactions implemented

$$DRM : CH_4 + CO_2 \iff 2H_2 + 2CO$$

$$RWGS : CO_2 + H_2 \iff CO + H_2O$$

$$MD : CH_4 \iff C + 2H_2$$

$$SG : C + H_2O \iff CO + H_2$$

$$BR : C + CO_2 \iff 2CO$$

  - Kinetics: Homogenous and Discrete reaction rate expressions

$$R_1 = \frac{k_1 K_{CO_2,1} K_{CH_4,1} P_{CH_4} P_{CO_2}}{(1 + K_{CO_2,1} P_{CO_2} + K_{CH_4,1} P_{CH_4})^2} \left(1 - \frac{(P_{CO} P_{H_2})^2}{K_{P_1} (P_{CH_4} P_{CO_2})}\right)$$

$$R_2 = \frac{k_2 K_{CO_2,2} K_{H_2,2} P_{CO_2} P_{H_2}}{(1 + K_{CO_2,2} P_{CO_2} + K_{H_2,2} P_{H_2})^2} \left(1 - \frac{(P_{CO} P_{H_2O})}{K_{P_2} (P_{CO_2} P_{H_2})}\right)$$

$$R_3 = \frac{k_3 K_{CH_4,3} \left(P_{CH_4} - \frac{P_{H_2}^2}{K_{P_3}}\right)}{\left(1 + K_{CH_4,3} P_{CH_4} + \frac{1}{K_{H_2,3}} P_{H_2}^{1.5}\right)^2}$$

$$R_4 = \frac{\frac{k_4}{K_{H_2O,4}} \left(\frac{P_{H_2O}}{P_{H_2}} - \frac{P_{CO}}{K_{P_4}}\right)}{\left(1 + K_{CH_4,4} P_{CH_4} + \frac{1}{K_{H_2O,4}} \frac{P_{H_2O}}{P_{H_2}} + \frac{1}{K_{H_2,4}} P_{H_2}^{1.5}\right)^2}$$

$$R_5 = \frac{\frac{k_5}{K_{CO,5} K_{CO_2,5}} \left(\frac{P_{CO_2}}{P_{CO}} - \frac{P_{CO}}{K_{P_5}}\right)}{\left(1 + K_{CO,5} P_{CO} + \frac{1}{K_{CO,5} K_{CO_2,5}} \frac{P_{CO_2}}{P_{CO}}\right)^2}$$

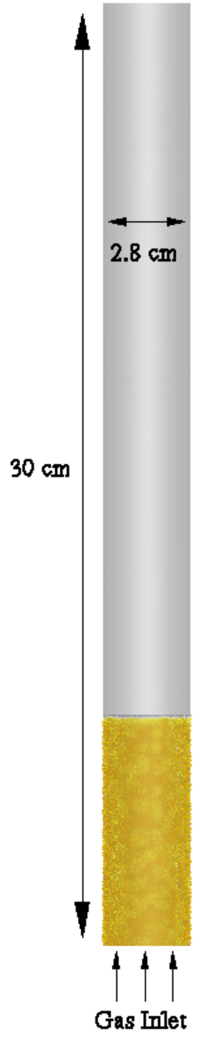

# Hydrogen Production with DRM

- **Animation shows CO and $H_2$ distribution in the reactor**
  - Greater $H_2$ to CO ratio – consistent with reaction pathways

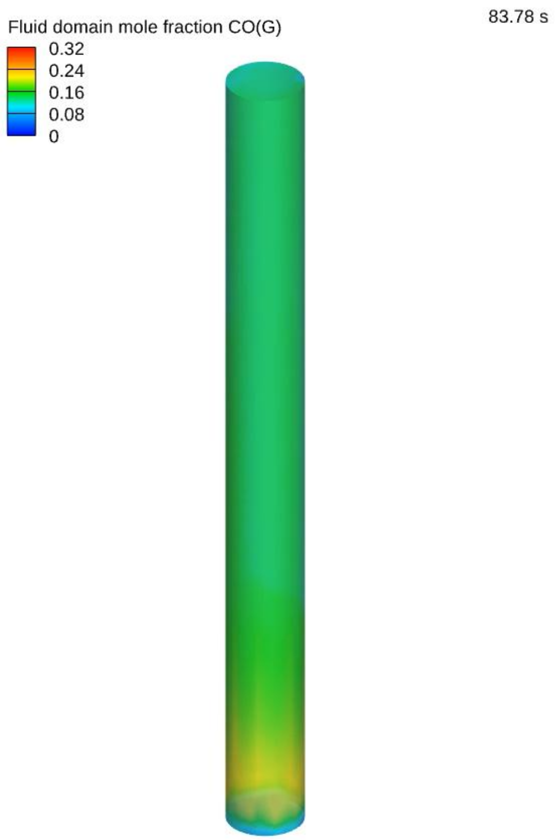


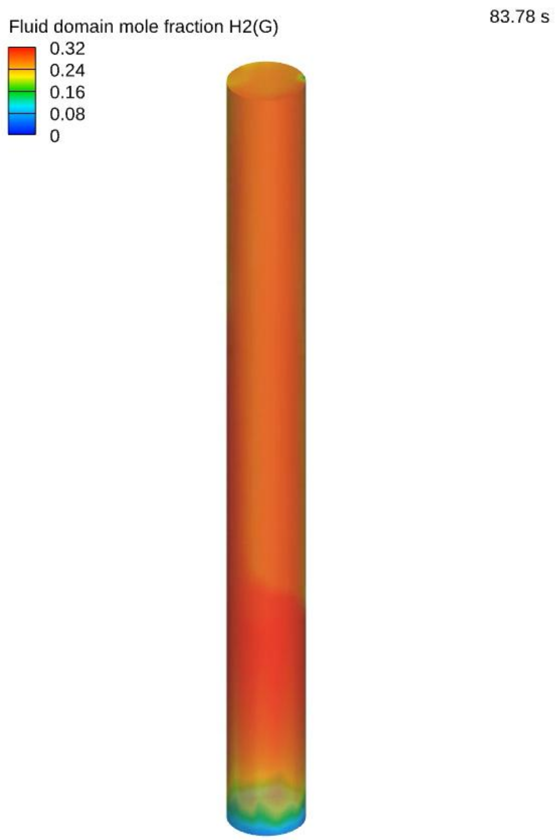


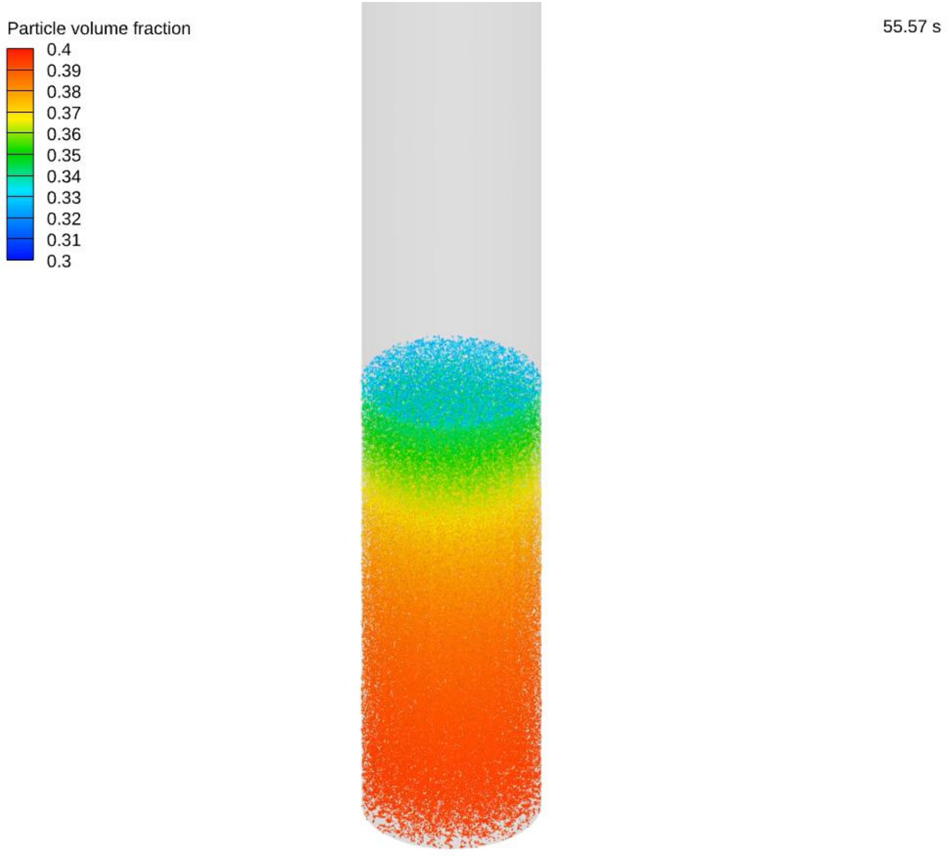


- **Catalyst Bed expansion visualized**

# Hydrogen Production with Molten Metal Bubble Column Reactor (MMBCR)

**Simulate Argon gas injection into a molten iron bath to evaluate bubble dynamics, targeting optimized interfacial area and residence time for low-carbon methane pyrolysis** (*based on work of Ngo et al.)*

- Barracuda Virtual Reactor Solution
  - MP-PIC framework applied to multiphase molten metal systems with compressible bubbles in an incompressible liquid bath
  - Bubble Coalescence and breakup modeled accounting for bubble size, relative velocity, volume fraction, turbulence, and liquid properties
- Value of Simulation
  - Predict bubble hydrodynamics in molten metal reactors without costly, hazardous experiments
  - Enable scale-up & optimization of $H_2$ production from methane decomposition in molten metal baths (e.g., Sn, Fe)
  - Gain unique insights into bubble coalescence, breakup, and dispersion not measurable in opaque molten system

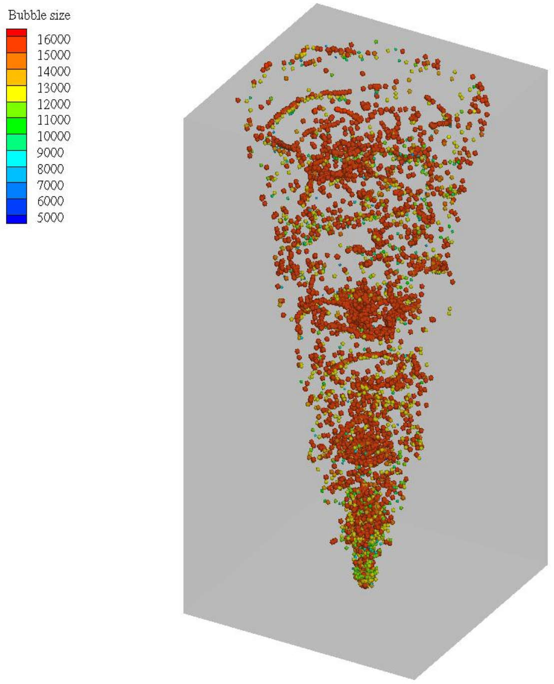

# Hydrogen Production with MMBCR

- Rectangular Reactor Domain
  - Filled with molten Fe @ 1250 c; Argon bubbles injected @ 2.5 mm3/sec
  - Grid count = 10,500 cells vs. 5 million cells for VOF model used by Ngo. et. al
- Maximum bubble size
  - Max bubble size limit needs to be set in Barracuda
    - Value estimated from based on work of Irons and Guthrie' 1978 and Ngo et. al' 2023
  - Coalescence factor controls probability of coalescence
    - Tuned based on experimental data for a single flow rate
- Bubble departure vs. orifice diameter
  - Figure shows linear relationship between bubble departure diameter and nozzle diameter (Islam et. al)

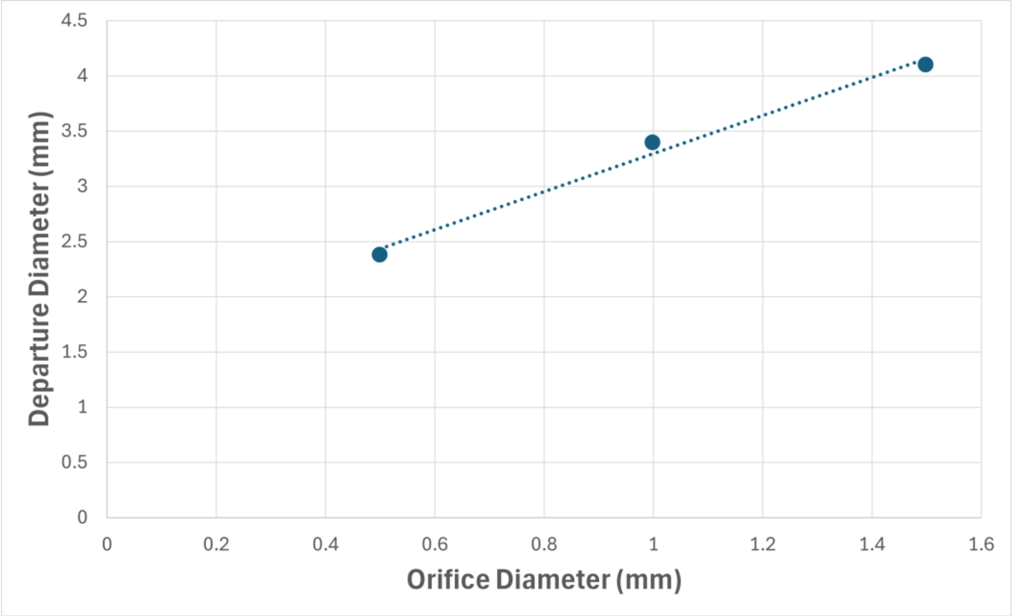

# Hydrogen Production with MMBCR

- Animation shows Argon bubbles raising up the reactor
  - Bubbles colored by their diameter

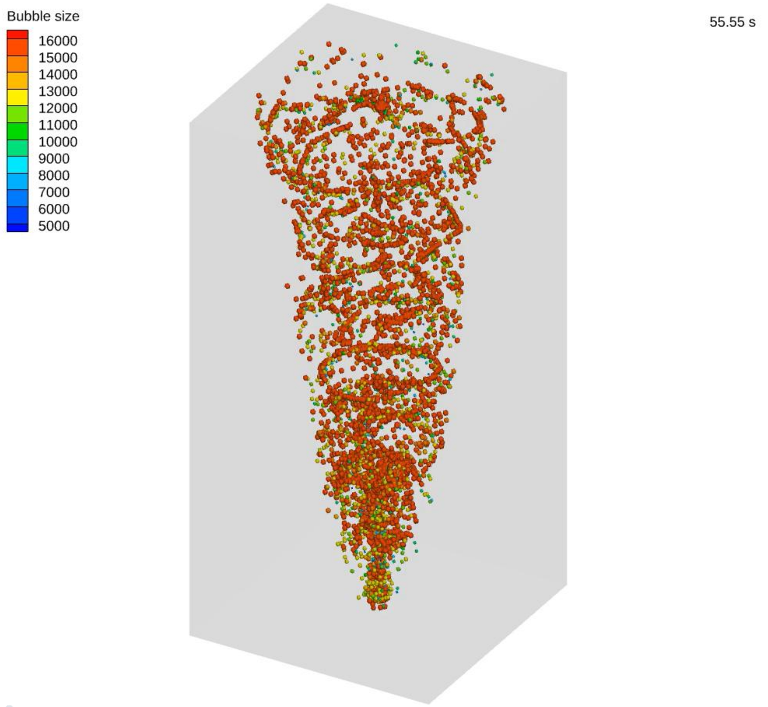


- Mean bubble diameter and drag coefficient at different flow rates compared with experimental and VOF-based simulation data
  - Comparable results obtained on a much coarser grid.
  - Computational time significantly less compared to VOF

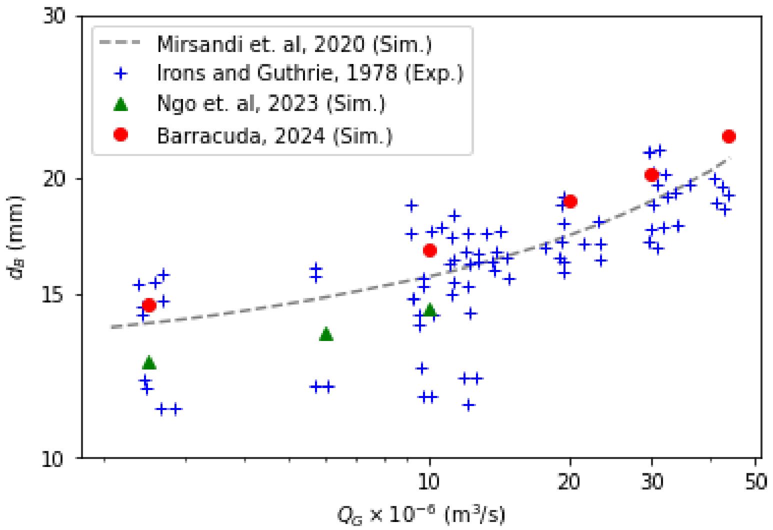


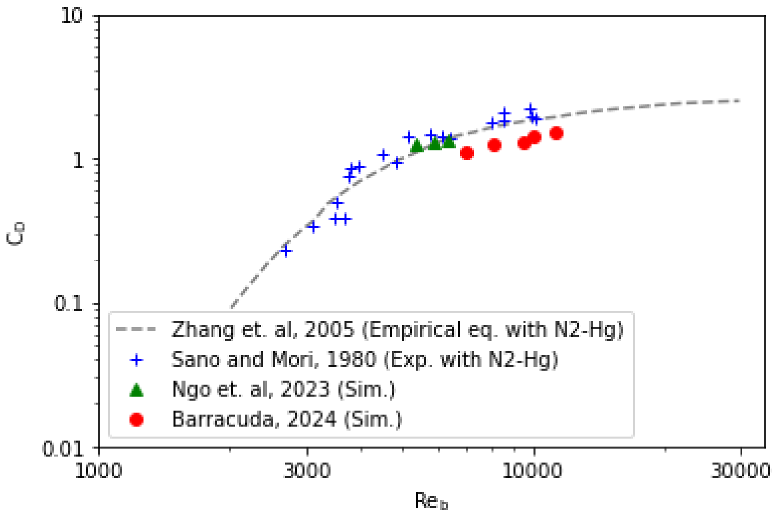

# DEMO

# Liquid – Solid Flows in Barracuda Virtual Reactor

# Hydraulic Fracturing and Proppant Transport

- **What is Hydraulic Fracturing?**
  - A stimulation technique where high-pressure fluid (slick water) is injected to fracture shale formations, exceeding the rock's tensile strength
  - Economic Impact: Drives 75% of U.S. natural gas production and 48% oil production (~$18.8B industry globally). Used in over 95% of new U.S. wells
- **The Critical Role of Proppant Transport**
  - Proppants are solid particles introduced to the fluid stream to physically hold fractures open once fluid pressure is removed
  - Conductivity: They create a semi-permeable superhighway for hydrocarbons to escape the rock and enter the wellbore
  - Optimization Value: Improving proppant distribution alone can increase well productivity by 20–50%.
  - Role of CFD: Because physical testing is impossible downhole, CFD is the primary tool for visualizing particle settling and optimizing transport strategies

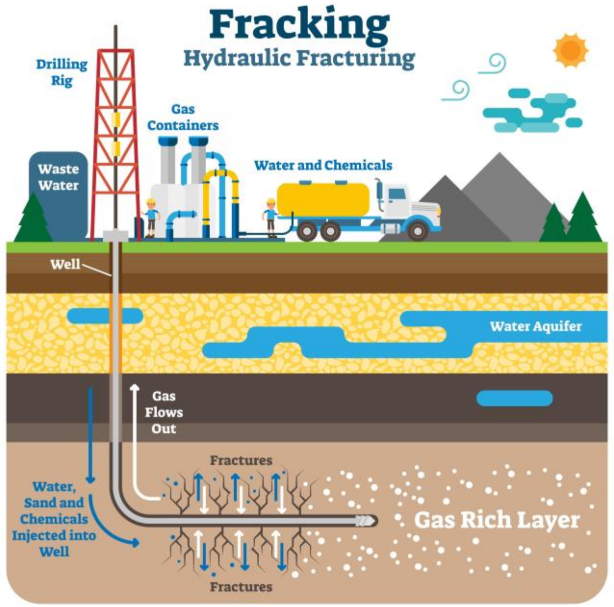


Ref: https://energiesmedia.com/10-best-performing-tips-for-successful-hydraulic-fracturing/

# Single Fracture Validation

- Based on experimental work of Zhou et. al, 2023
- BC Conditions:
  - Slick water injected 1.39m/sec; 2.5cP viscosity
  - 0.9% proppant concentration
  - 40/70 mesh size for the proppant assumed- Full PSD modeled
- Non-Newtonian Drag model: To account for shear thinning hydrodynamics of slick water

$$\tau_{xy} = K\left(\frac{du}{dy}\right)^n$$

*Where $K$ is consistency index*
*$n$ = power law exponent*

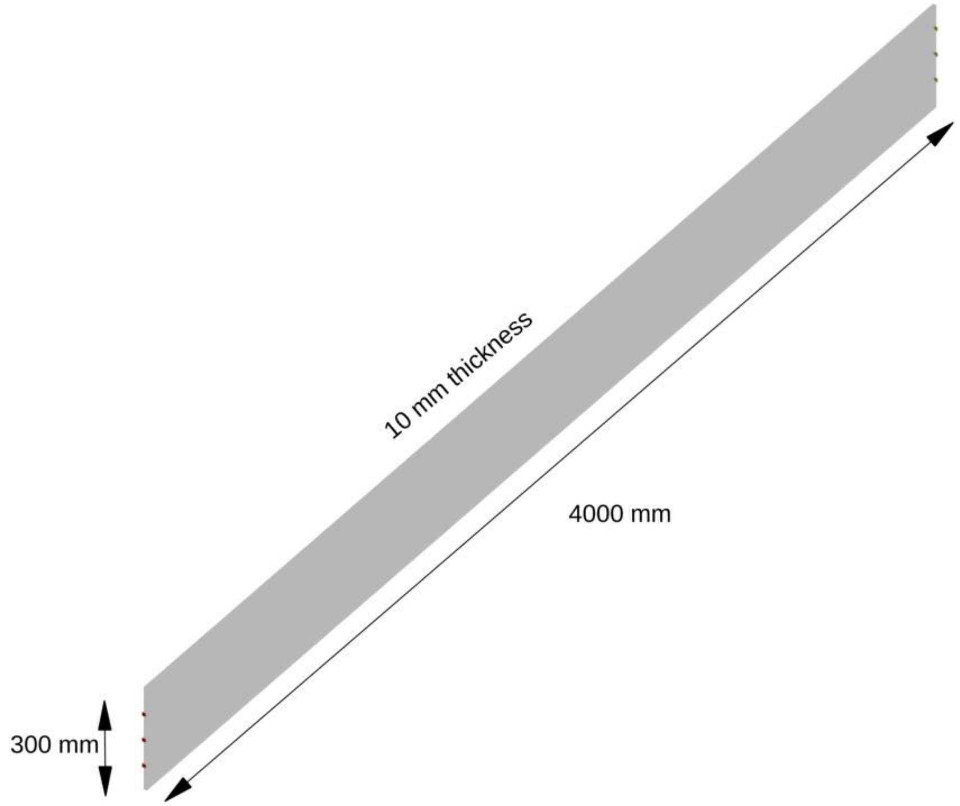


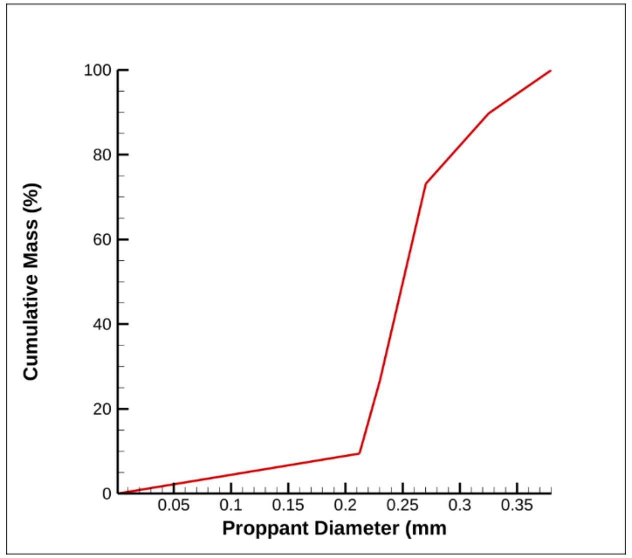

# Single Fracture Validation

- Proppant transport animation shows proppant volume, velocity and age

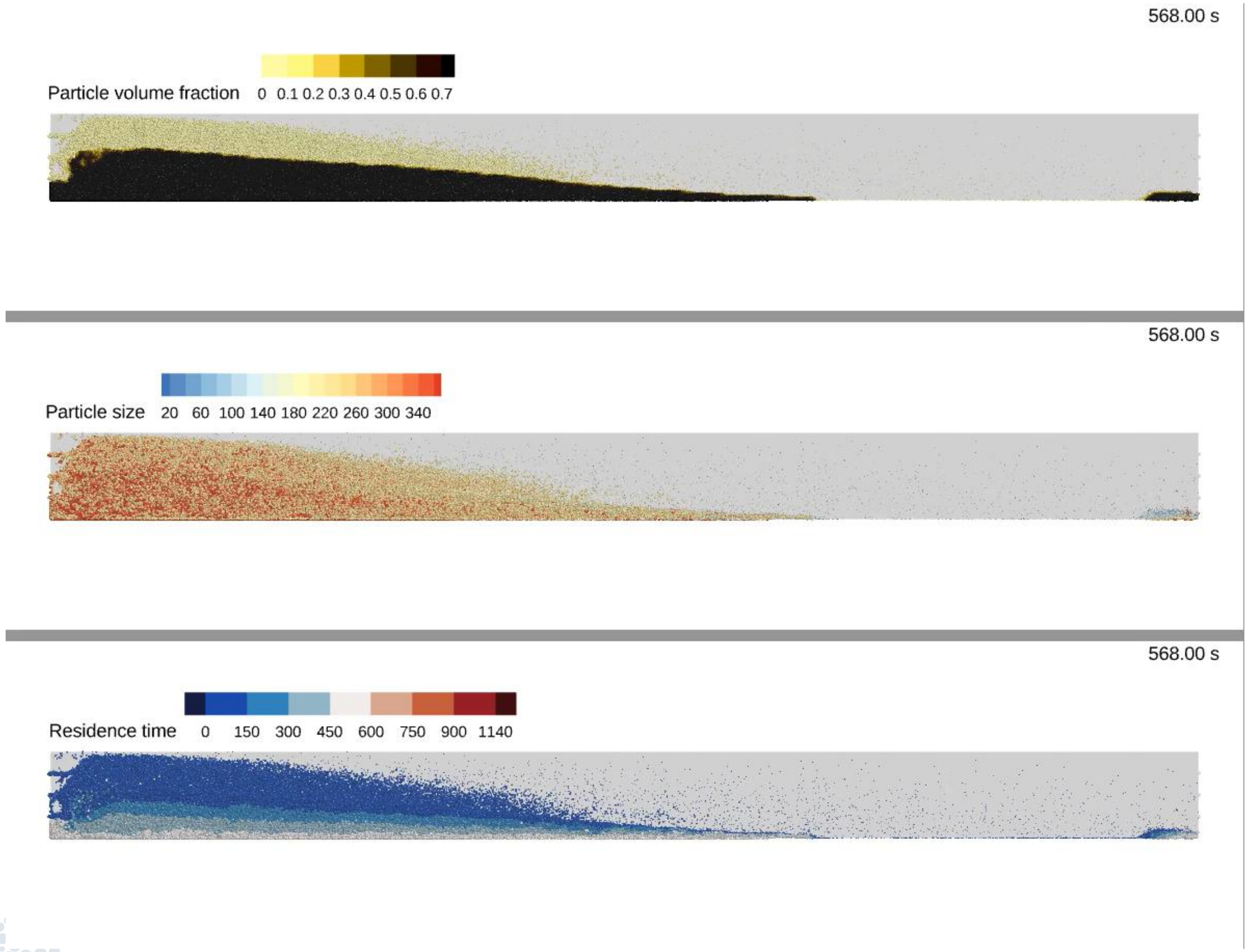


- Bed profile and height show a good match with the experiment

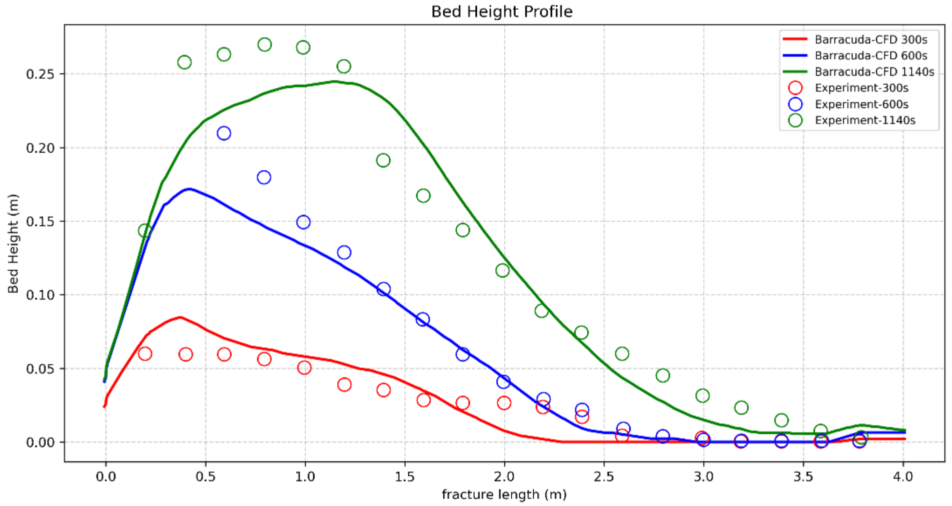


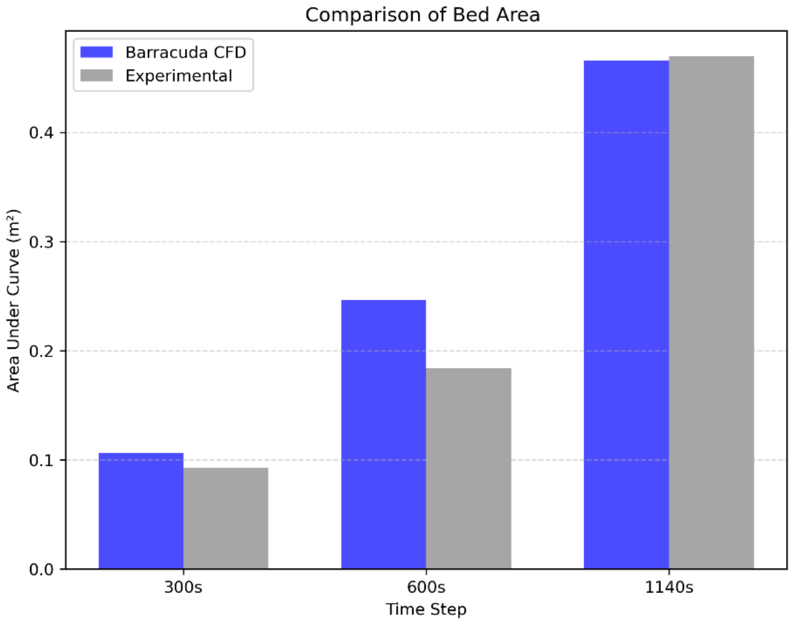

# Proppant Transport in Multiple Field Scale Fractures

**Barracuda is used to simulate proppant transport in field scale realistic sized domains**

**Proppant placement in 3 different sized fractures is studied**

- Fracture spacing is varied
  - Fracture lengths vary based on fracture spacing to account for stress shadow effect
  - Fracture width non-uniform (Tapered fracture domain)
- Different slurry pumping flow rates analyzed

# Multiple Fracture Domains

5m Spacing

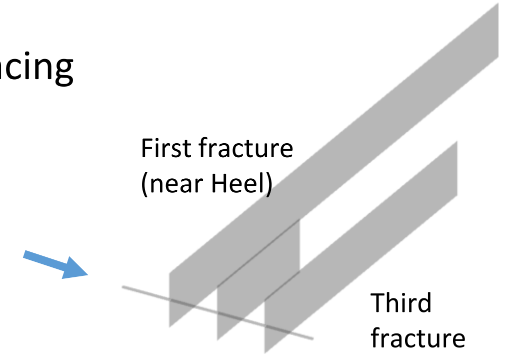


| | Fracture gap - m (ft) | Length -m (ft) | Thickness [in] | | Height - m (ft) |
|---|---|---|---|---|---|
| | | | Start | End | |
| First (Heel) | 5 (16.4) | 60 (196.8) | 1 | 0.6 | 6 (19.6) |
| Second | | 15 (49.2) | 1 | 0.4 | 6 (19.6) |
| Third (Toe) | | 35 (114.8) | 1 | 0.6 | 6 (19.6) |

10m Spacing

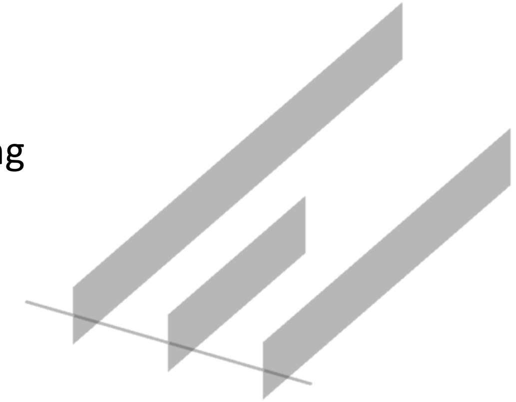

| | Fracture gap - m (ft) | Length - m (ft) | Thickness [in] | | Height - m (ft) |
|---|---|---|---|---|---|
| | | | Start | End | |
| First (Heel) | 10 (32.8) | 60 (196.8) | 1 | 0.6 | 6 (19.6) |
| Second | | 25 (82.0) | 1 | 0.5 | 6 (19.6) |
| Third (Toe) | | 45 (147.6) | 1 | 0.6 | 6 (19.6) |

20m Spacing

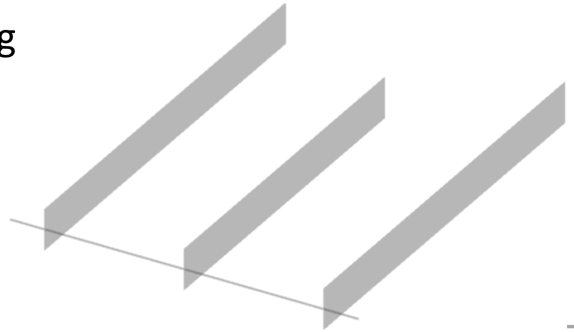

| | Fracture gap - m (ft) | Length -m (ft) | Thickness [in] | | Height - m (ft) |
|---|---|---|---|---|---|
| | | | Start | End | |
| First (Heel) | 20 (65.6) | 60 (196.8) | 1 | 0.6 | 6 (19.6) |
| Second | | 50 (164.0) | 1 | 0.6 | 6 (19.6) |
| Third (Toe) | | 60 (196.8) | 1 | 0.6 | 6 (19.6) |

# Multiple Fractures Simulations Execution

- Proppant pumping rate
  - 30 bbl/min
  - 45 bbl/min
- Well toe end closed
- Proppant and fluid allowed to leave fracture toe end
- 40/70 mesh sand
  - Full PSD defined

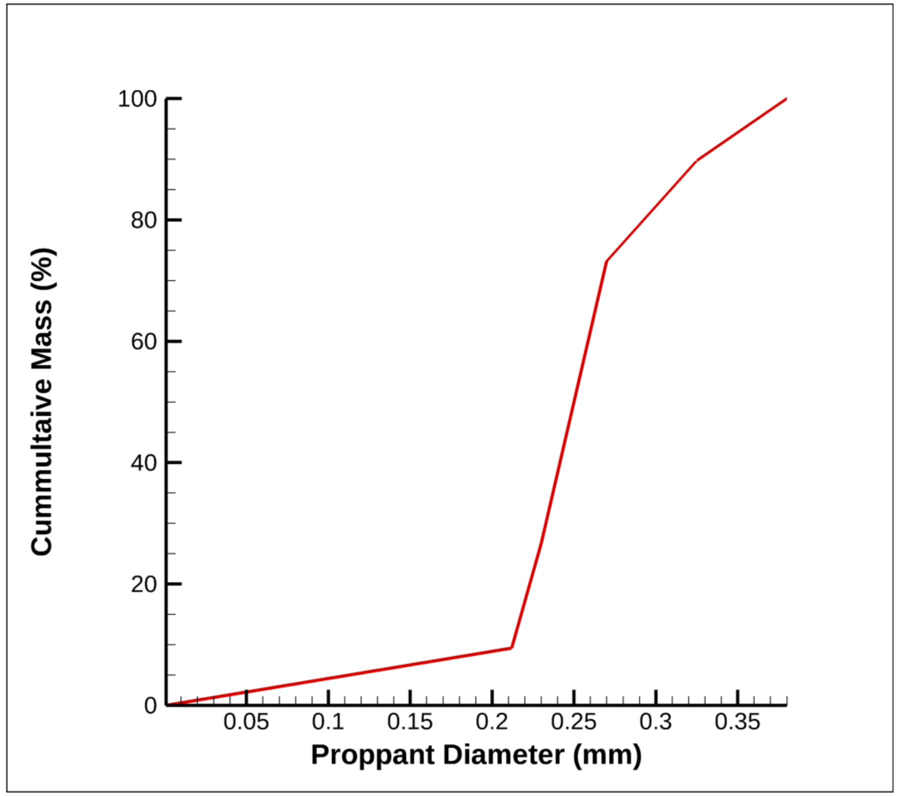


**Simulations were run for a physical pumping time of 20 mins**

- Average simulation clock time = 17 hours
- 1 GPU card used - NVIDIA RTX 6000

# Influence of Spacing on Proppant Placement

- Proppant pumping rate = 30 bbl/min
- 40/70 mesh sand
- 20 m spacing case sees no proppant injection into the toe end fracture

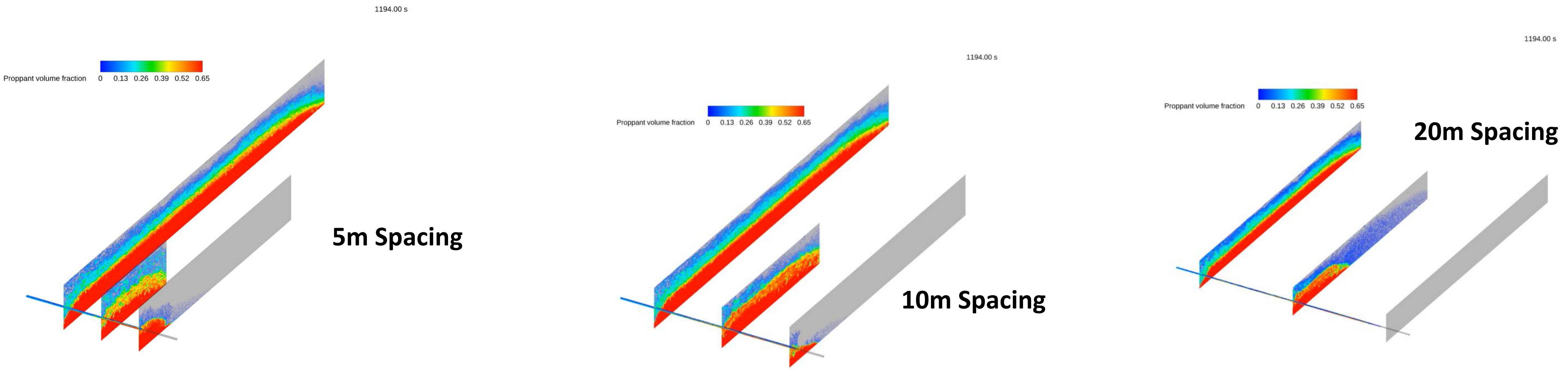

# Influence of Spacing on Proppant Placement

- Tight Spacing (5m): Stress Shadowing acts as back-pressure on the first fracture, forcing more slurry downstream
- Wide Spacing (20m): Pipe Friction makes travel to the second fracture harder, so fluid takes the easy path into the first fracture
- Toe fracture is starved in all cases: Momentum loss

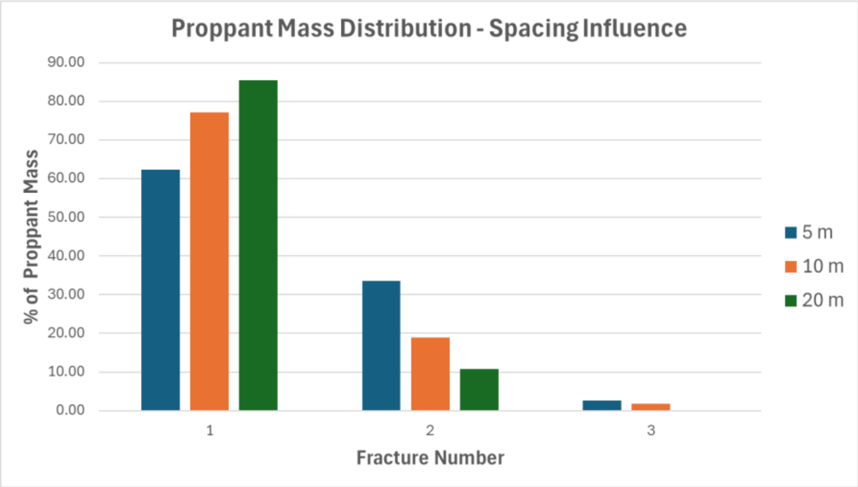


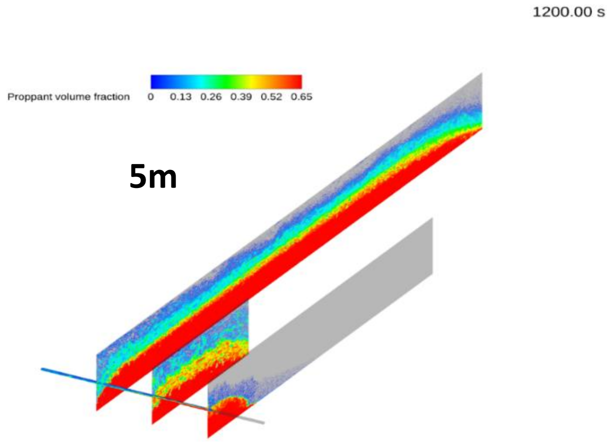


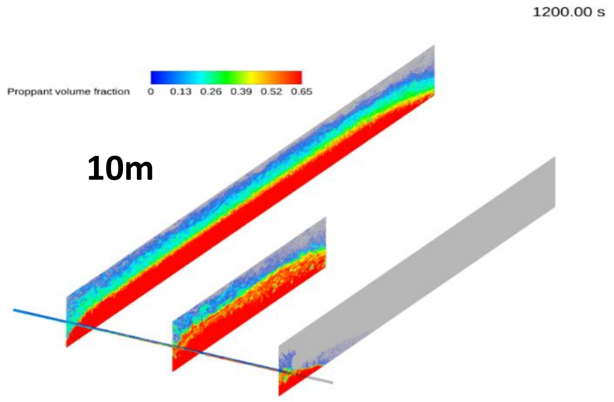


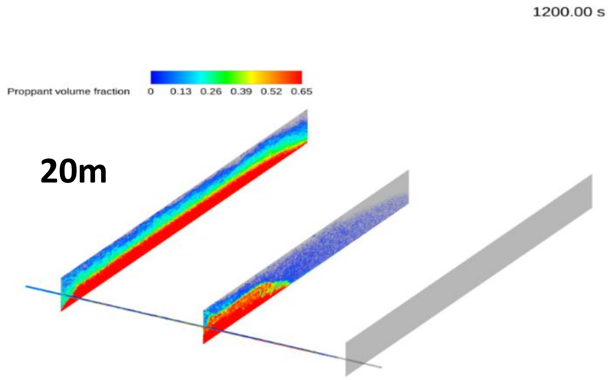

# Influence of Flow Rates on Proppant Placement

- Can increasing the flow to 45 bbl/min place more proppant in the middle and toe end fractures?
- Comparing 10 m spacing case

30 bbl/min

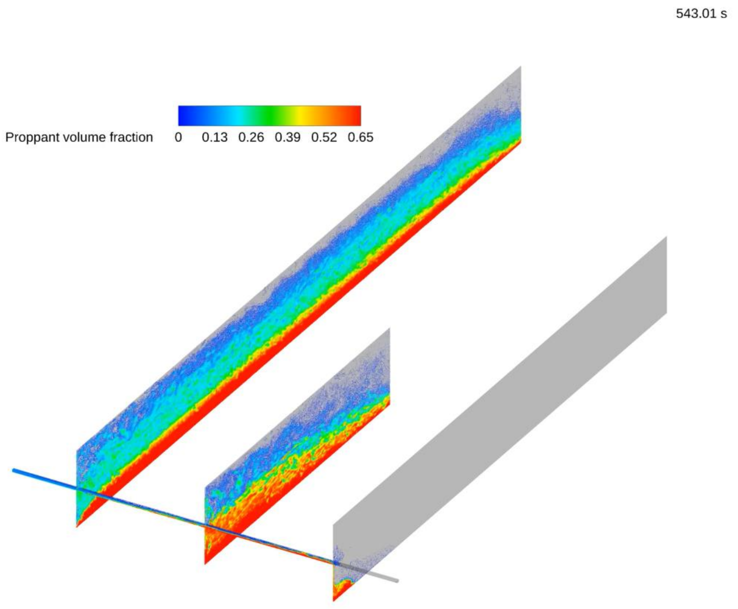


45 bbl/min

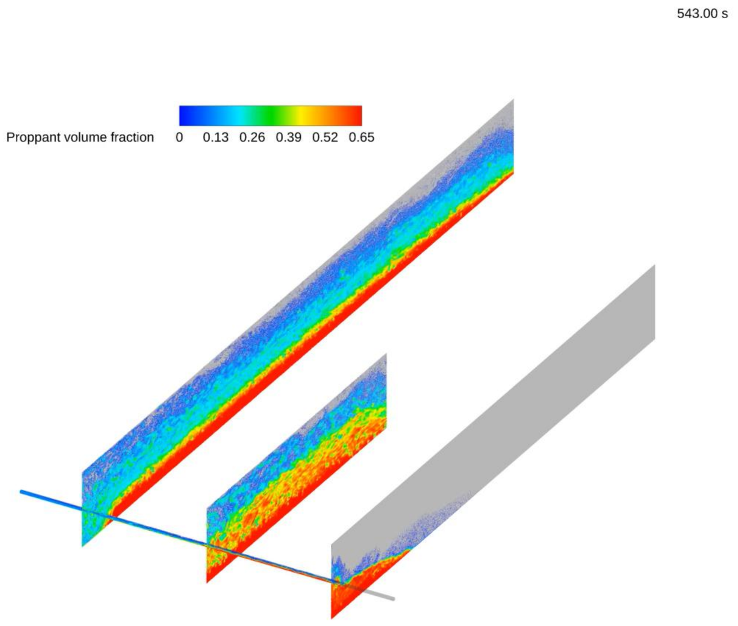

# Influence of Flow Rates on Proppant Placement

- High Rate (45 bbl/min): Inertia carries particles past the first opening, forcing them further downstream
- Low Rate (30 bbl/min): Low Velocity allows the first fracture to easily capture the slurry before it can travel further
- Toe fracture starvation persists

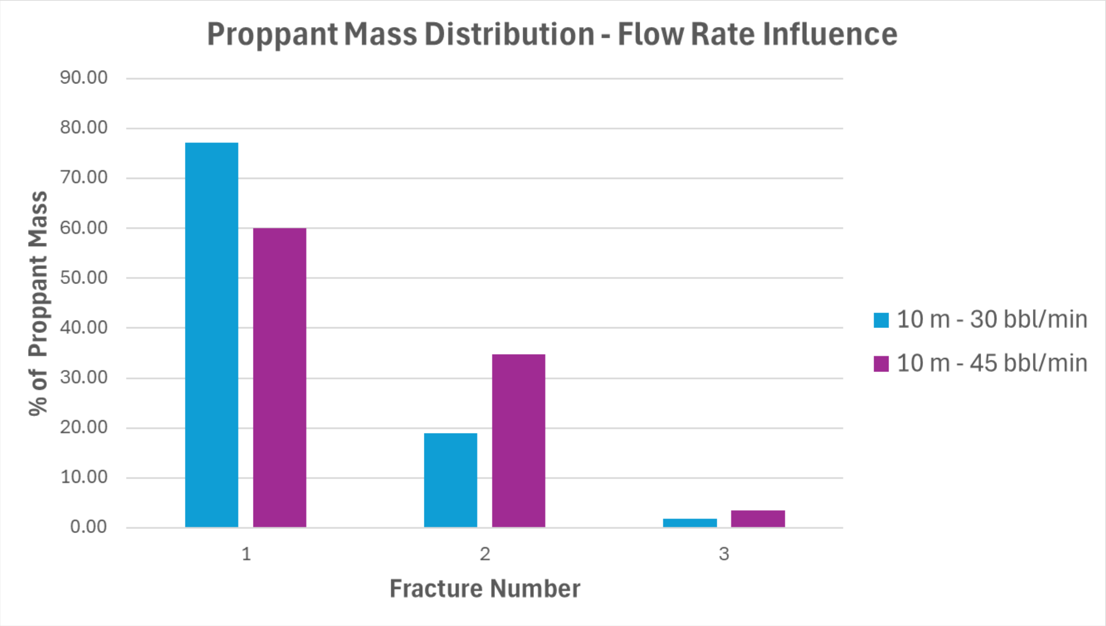


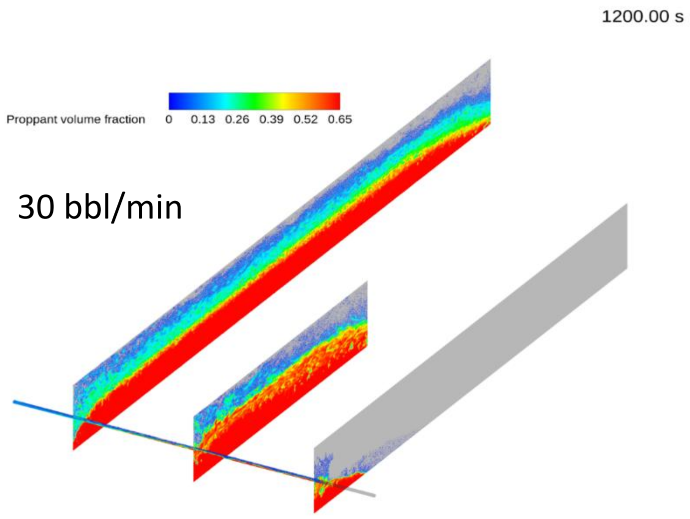


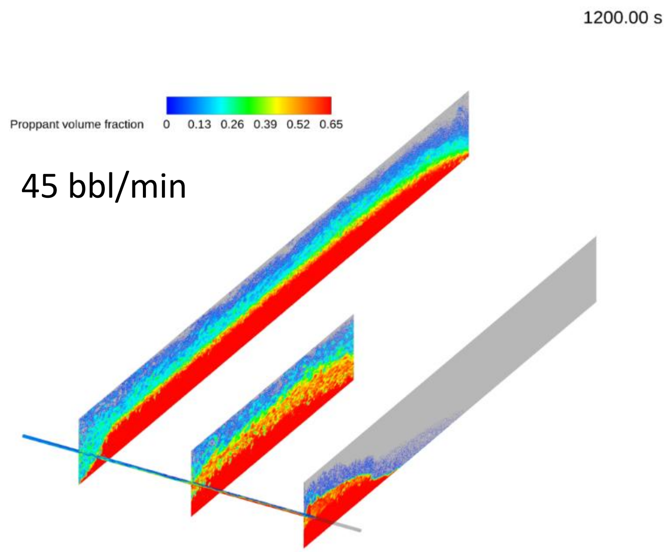

# Sand Screens in Oil & Gas Completions

## The Problem & Solution

- Formation sand and proppant flowback during production erode equipment, reduce fracture conductivity, and force costly interventions
- Sand screens are downhole filters that mechanically block particles larger than the slot width;
  - smaller fines pass through, while coarse grains bridge on the screen surface and stabilize the bed behind them

- **Barracuda Solution**
  - Screen slot widths (100–250 µm) are $10^4$–$10^5$× smaller than the simulation domain
    - direct geometric resolution is computationally prohibitive
  - Barracuda's baffle model represents the screen as a filtering surface with particle size-dependent passing probability
  - MPPIC naturally tracks local particle concentration over time
    - Particle bridging behavior emerges from stress modeling physics

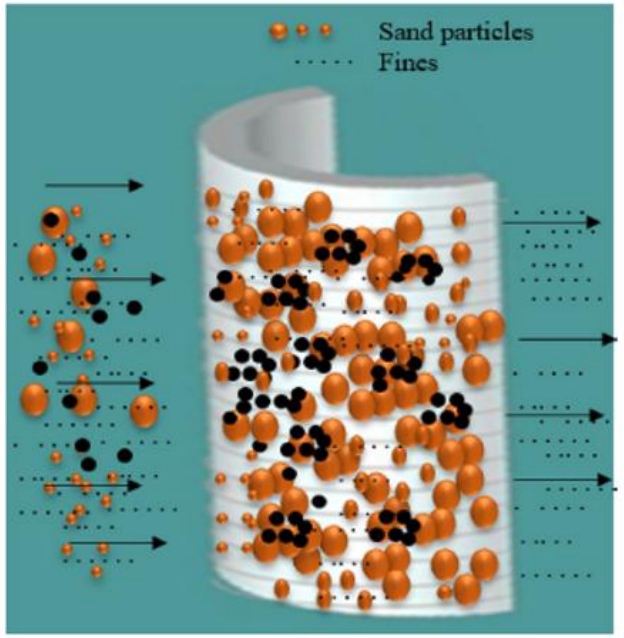


Ref: https://link.springer.com/article/10.1007/s13202-022-01467-4

# Sand Screen Model

## Flow through the wellbore annulus passes through the standalone screen modeled as a baffle

- Baffle can be used to model a wire-wrap screen, woven-metal-mesh or premium screen etc.
- Baffle takes particle passing probability as an input
- Particle passing probability can be tuned to match type of sand screen,
  - For e.g. screen size based on sand retention test data (e.g., Mondal et. al, 2011, 2012)
- Different sized sand screen can have different passing probabilities

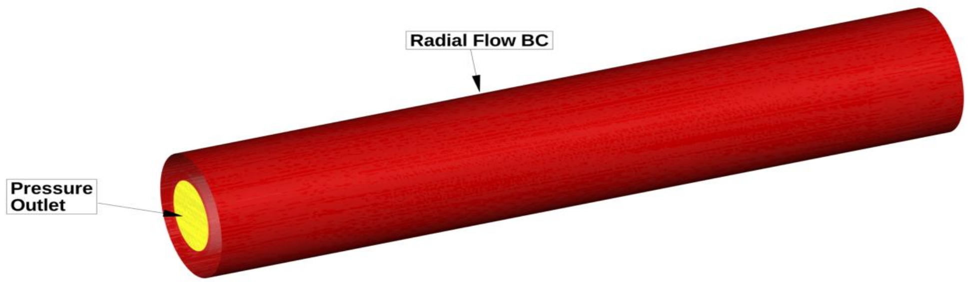


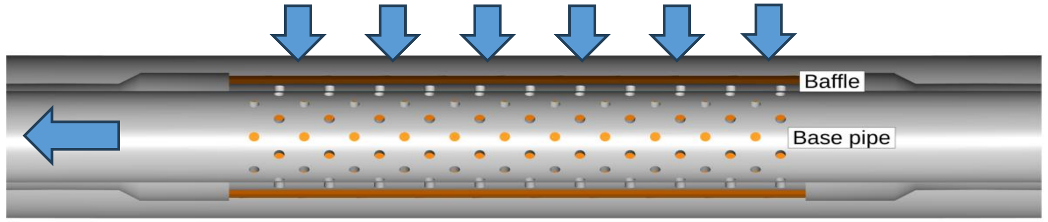


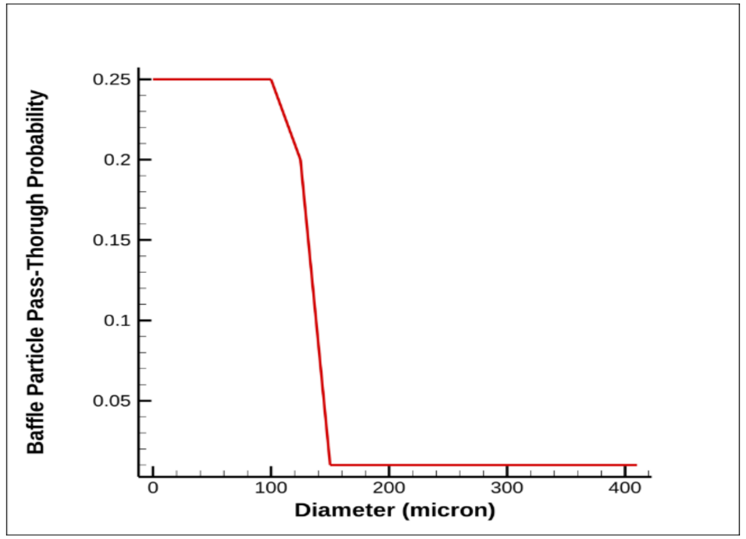


Baffle Particle Passing Probability

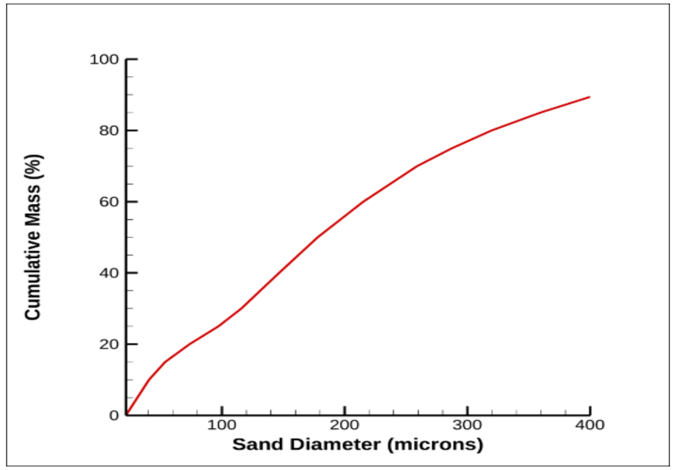


Sand PSD

# Sand Screen Filtering

**Animation shows particles filtered based on baffle passing probability**

**Sand inlet and out PSD quantified through histograms**

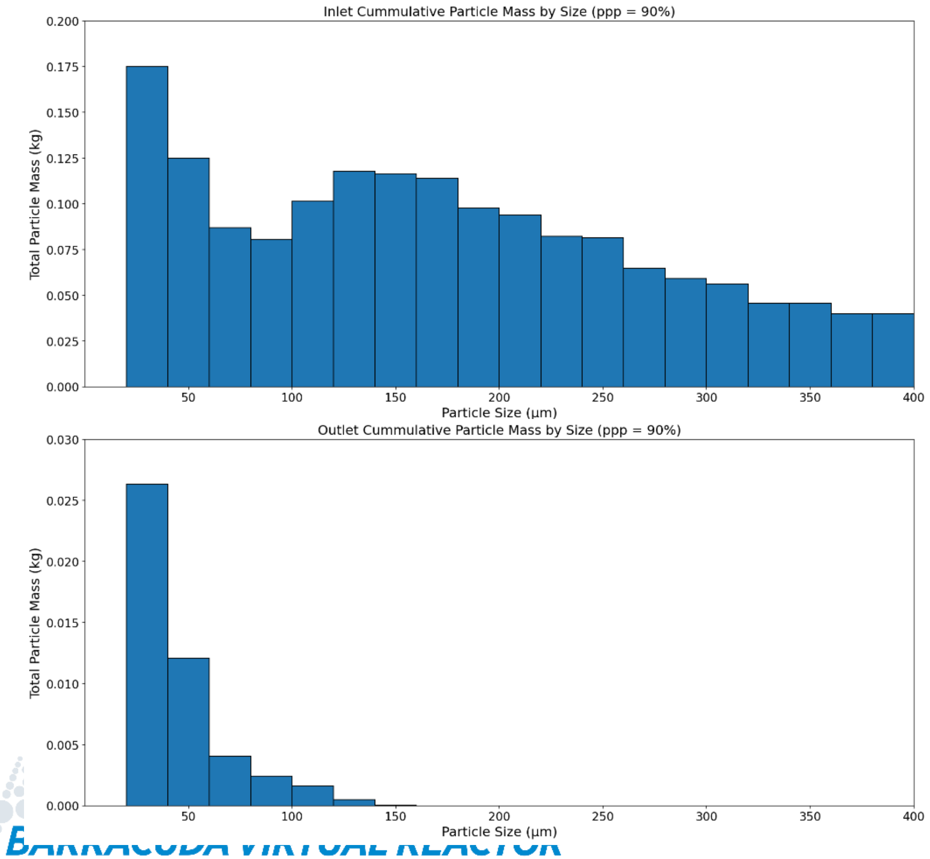


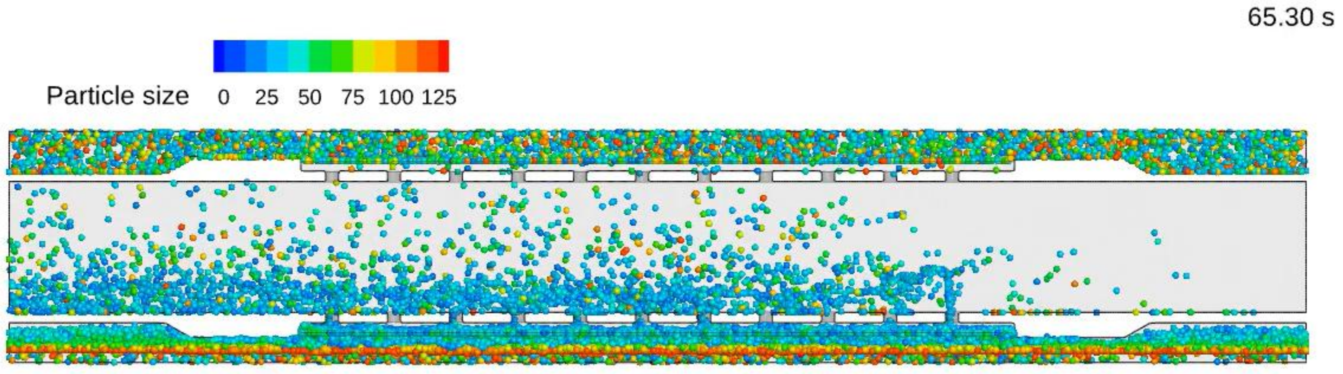


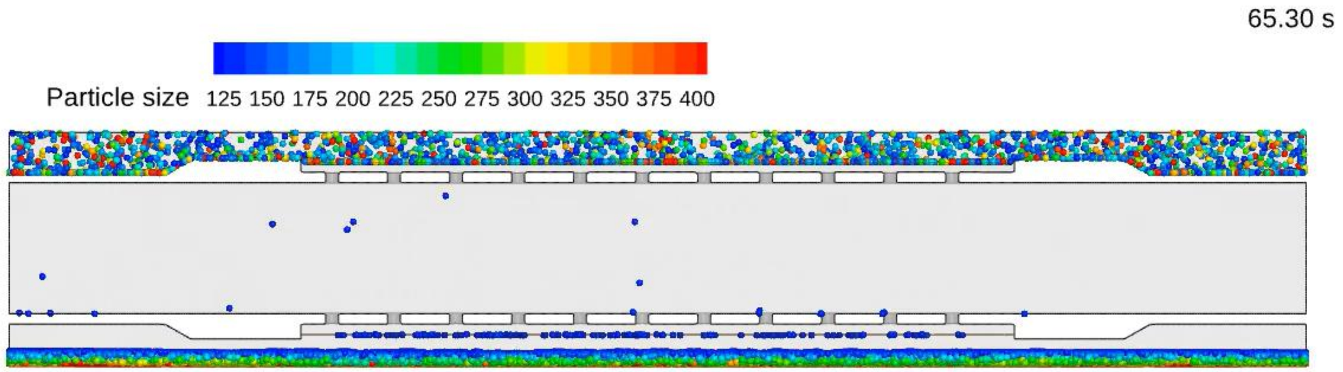


**Barracuda can be used for sand screen selection, performance over real world systems**

# Thank you!

**Download and adapt Barracuda Virtual Reactor Application Models for your own engineering analysis**

**https://cpfd-software.com/resource/application-models/**